Single-Molecule Imaging

DOI: 10.1002/anie.201205247

Single-Molecule Visualization of the Hybridization and Dissociation of Photoresponsive Oligonucleotides and Their Reversible Switching Behavior in a DNA Nanostructure**

Masayuki Endo, Yangyang Yang, Yuki Suzuki, Kumi Hidaka, and Hiroshi Sugiyama**

Direct observation of the hybridization and dissociation of a double-stranded DNA at molecular resolution is a challenging and fundamental issue for nanoscience and molecular imaging. Single molecules can show different characteristics, which are hidden when observed in the ensemble state under bulk conditions. Individual molecules can behave heterogeneously, depending on the physical state of the molecules and the local environment around them.[1–3] Single enzymes and chemical reactions can now be visualized and analyzed on DNA nanostructures using various analysis methods.[4–9] Direct visualization of the hybridization and dissociation of a single duplex would be quite fascinating, however, there is currently no method available to observe it under physiological conditions. We have recently developed a single-molecule observation platform for DNA-binding proteins and enzymes and DNA structural changes using a DNA-origami nanostructure and high-speed atomic force microscopy (AFM).[10–13]

Herein, we imaged single-molecule hybridization and dissociation of a double-stranded DNA using photoresponsive domains containing azobenzene moieties.[14,15] The photoresponsive domain can hybridize with the corresponding pseudocomplementary photoresponsive counterpart in the *trans*-form of the azobenzene moiety and dissociate in the *cis*-form by photoirradiation of a different wavelength.[15] The *trans*-form of azobenzene-modified oligonucleotides can hybridize using a pair of pseudocomplementary sequences, in which one contains three azobenzene moieties (**X3**) and the other contains four (**X4**) (Figure 1). Two double-stranded DNAs (dsDNA) with photoresponsive domains at the center were placed in the cavity (approximately 40 × 40 nm) of the DNA frame.[10–12] The single-molecule hybridization and dissociation can be identified by a global structural change of the two dsDNAs as an X-shape and as a separated-shape in the DNA frame, respectively (Figure 1 a).

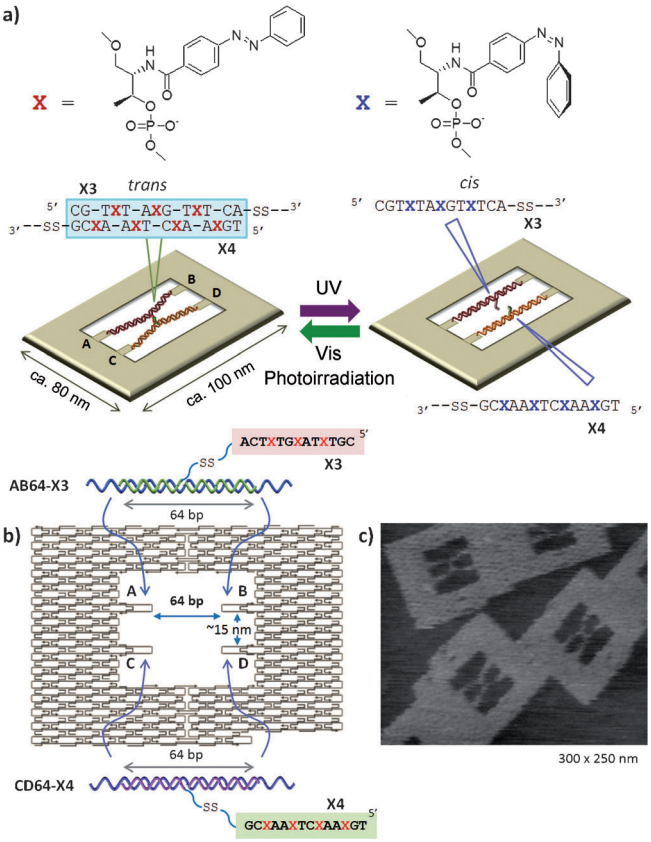

Figure 1. Single-molecule observation system for the hybridization and dissociation of a pair of photoresponsive oligonucleotides. a) In the *trans*-form, two photoresponsive oligonucleotides hybridize to form a duplex. In the *cis*-form, after UV irradiation, the two oligonucleotides dissociate. Two dsDNAs containing these photoresponsive domains were placed within the DNA frame structure. b) Two different dsDNAs containing different photoresponsive domains (**X3** and **X4**) were connected to the specific sites (**A**-**B** and **C**-**D**) in the DNA frame using the corresponding ssDNA sticky ends. c) AFM image of the assembled structure.

[*] Dr. M. Endo, Prof. H. Sugiyama
Institute for Integrated Cell-Material Sciences (WPI-iCeMS)
Kyoto University
Yoshida-ushinomiyacho, Sakyo-ku, Kyoto 606-8501 (Japan)
E-mail: endo@kuchem.kyoto-u.ac.jp
hs@kuchem.kyoto-u.ac.jp
Y. Yang, Dr. Y. Suzuki, K. Hidaka, Prof. H. Sugiyama
Department of Chemistry, Graduate School of Science
Kyoto University
Kitashirakawa-oiwakecho, Sakyo-ku, Kyoto 606-8502 (Japan)
Dr. M. Endo, Prof. H. Sugiyama
CREST, Japan Science and Technology Corporation (JST)
Sanbancho, Chiyoda-ku, Tokyo 102-0075 (Japan)

[**] We thank Prof. H. Asanuma (Nagoya University) for valuable advice and comments. This work was supported by Core Research for Evolutional Science and Technology (CREST) of JST and Grant-in-Aid for Scientific Research form MEXT (Japan). Financial support from Nagase Science and Technology Foundation to M.E. is also acknowledged. Y.Y. was supported by China Scholarship Council (CSC).

Supporting information for this article is available on the WWW under http://dx.doi.org/10.1002/anie.201205247.

We prepared oligonucleotides containing the photoresponsive domain (Figure 1a and Supporting Information, Scheme S1) and confirmed their photoisomerization performance (Supporting Information, Figure S2). The azobenzene-modified strands **X3** and **X4** with thiol at the 3′-termini were connected to the 32-mer single-stranded DNAs (ssDNAs), with a thiol at the 5′-terminus through a disulfide bond. Following purification by HPLC (Figure S1), the ssDNAs containing the photoresponsive domain and the corresponding unmodified ssDNAs were annealed with their complementary DNA strands, which had ssDNA overhangs at both ends for incorporation into the DNA-origami frame (Figure 1b and Table S1).

After assembling two dsDNAs (**AB64-X3** and **CD64-X4**) containing the corresponding photoresponsive domains, these dsDNAs were incorporated into the preassembled DNA frame in a solution containing 20 mM Tris buffer (pH 7.6), 10 mM $MgCl_2$, and 1 mM EDTA, and the mixture was annealed from 40 °C to 15 °C at a rate of −0.5 °C min^{-1}. The assembled structures were imaged using AFM. Two dsDNAs placed in the DNA frame were found to be connected at the center by hybridization of the photoresponsive domains (X-shaped structure; Figure 1c). In addition, the hybridization of the photoresponsive domains was clearly visualized between the two dsDNAs at the center. The length of the hybridized photoresponsive domains was measured to be 9–11 nm, which corresponds to the total length of a 17 bp duplex (5.8 nm) plus the two likers (4.7 nm; Figure 1c and Figure S3). After assembly, most (approximately 80%) of the structures formed an X-shape (Figure 2a), indicating that the photoresponsive domains in the *trans*-form were hybridized when the two dsDNAs were incorporated into the DNA frame.

Initially, the assembled DNA frame was irradiated with UV light in solution. After UV irradiation (Asahi spectra MAX-303; $\lambda = 350$ nm band pass filter) for 15 minutes at 25 °C, the sample was imaged using AFM. Following irradiation, the separated-shape in the DNA frame was observed, and the percentage of separated-shapes increased from 16% to 26% (Figure 2b). These results showed that the two hybridized photoresponsive domains dissociated upon isomerization of the *trans*-form to the *cis*-form. Furthermore, when the UV irradiated samples were treated with visible-light irradiation ($\lambda =$ 450 nm band pass filter) for 15 min at 25 °C, the percentage of X-shapes increased from 64% to 74% (Figure 2c); this showed the *cis*- to *trans*-form isomerization and subsequent hybridization. The proportion of the two shapes clearly shows that the decrease of the percentage of X-shapes corresponds to an increase in the percentage of separated-shapes (Figure 2d and Table S2). These results indicate that the photoresponsive domains placed within the DNA frame work as expected in solution with photoirradiation at different wavelengths.

Because hybridization and dissociation of the photoresponsive oligonucleotides should depend on the reaction temperatures, we carried out photoirradiation in a temperature-controlled bath at three different temperatures, 25, 30,

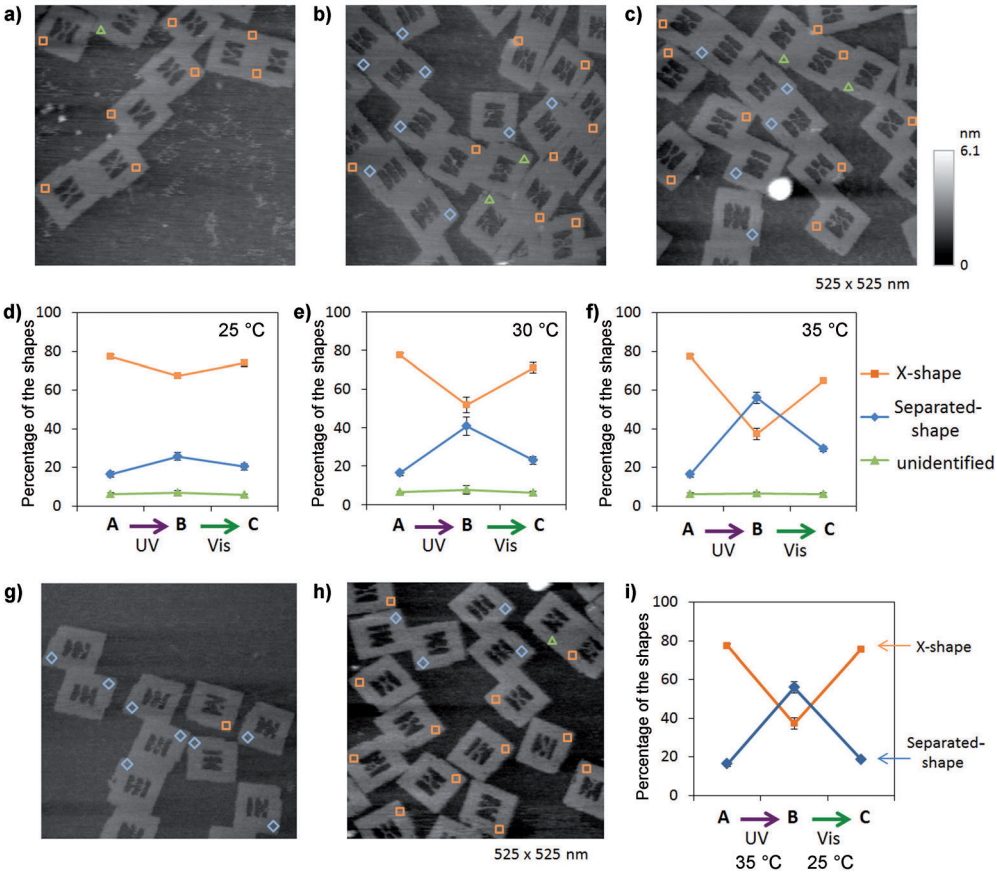

Figure 2. Photoinduced dissociation and hybridization of photoresponsive oligonucleotides in the nanostructure. AFM images of DNA frames a) after the introduction of two dsDNAs; b) after UV irradiation for 15 min at 25 °C; c) after visible-light irradiation for 15 min at 25 °C of the sample from (b). X-shape = orange rectangle; separated-shape = blue diamond; unidentified shapes = green triangle. d–f) Temperature-dependent percentage of X-shapes and separated-shapes after UV and visible-light irradiation at 25 °C (d), 30 °C (e), and 35 °C (f). A = after assembly, B = after UV irradiation, and C = after UV then visible-light irradiation. g,h) Temperature-controlled photoirradiation for the effective dissociation and hybridization of the photoresponsive domains. AFM images after UV irradiation at 35 °C (g) and with subsequent visible-light irradiation at 25 °C (h). i) Percentage of X-shapes and separated-shapes under the specified photoirradiation conditions.

and 35 °C (Figure S4) and assessed the formation of the separated-shapes (Figure 2 d–f and Table S2). The higher reaction temperature showed better conversion to the separated-shape as compared with incubation at lower temperatures, and the percentage of separated-shapes reached 56 % at 35 °C. The efficiency for the separation of dsDNAs in the DNA frame showed dependence on the reaction temperature. Higher temperatures are favorable for the dissociation of duplexes, and thus should be needed for higher dissociation efficiency of the hybridized photoresponsive oligonucleotides in the DNA frame. These results are also consistent with the thermal properties of the intact photoresponsive oligonucleotides reported previously.[15] Successive visible-light irradiation to form the X-shape was also performed using the UV-irradiated samples at the three different temperatures. At the higher temperatures, the separated-shapes did not completely return to the initial X-shape, meaning that a lower temperature is better for the hybridization of the dissociated photoresponsive oligonucleotides. From these results, we tried producing efficient dissociation and hybridization of the duplexes by controlling the reaction temperature during photoirradiation. We used 35 °C for UV irradiation and 25 °C for successive visible-light irradiation; AFM images of these products are shown in Figure 2 g,h. The percentage of X-shapes following visible-light irradiation reached 76 %, which indicates a complete return to the initial state (77 %) (Figure 2 i). This result clearly shows that a lower temperature promotes the hybridization of the photoresponsive oligonucleotides, even when incorporated into the nanostructure.

We further characterized the dissociation and hybridization processes using high-speed AFM imaging.[16] According to a previous report,[15] the melting temperature of the duplexes with the photoresponsive domains is over 50 °C, thus our system at 25 °C was suitable for observing both hybridization and dissociation induced by photoirradiation. Before observing the photoresponses within the DNA frame, we examined the photoisomerization of azobenzene moieties in the oligonucleotide using the photoirradiation system equipped on the AFM instrument. The changes in the UV/Vis spectra under the different irradiation conditions (Figure S6) showed that this photoirradiation system can be used for the photoisomerization of the oligonucleotides. A sample of DNA frames containing photoresponsive domains was adsorbed on a mica surface. For the *trans*- to *cis*-form isomerization, UV irradiation ($\lambda = 330$–380 nm) was performed on the AFM stage during scanning. The dissociation of the two dsDNAs during UV irradiation was imaged at the single-molecule level (Figure 3 and Movie S1). In the successive AFM images, the time of the structural change from X-shape to separated-shape (30–70 s) varied depending on the individual DNA frames. Some dsDNAs within the DNA frame did not respond to photoirradiation, which may be attributed to their strong contact with the mica surface, resulting in suppression of the movement of the dsDNAs in the frame.

We next examined the hybridization of the dissociated photoresponsive domains during AFM scanning; a sample irradiated with visible light ($\lambda = 440$–470 nm) on the AFM stage was used for this observation (Figure S7 and Movie S2).

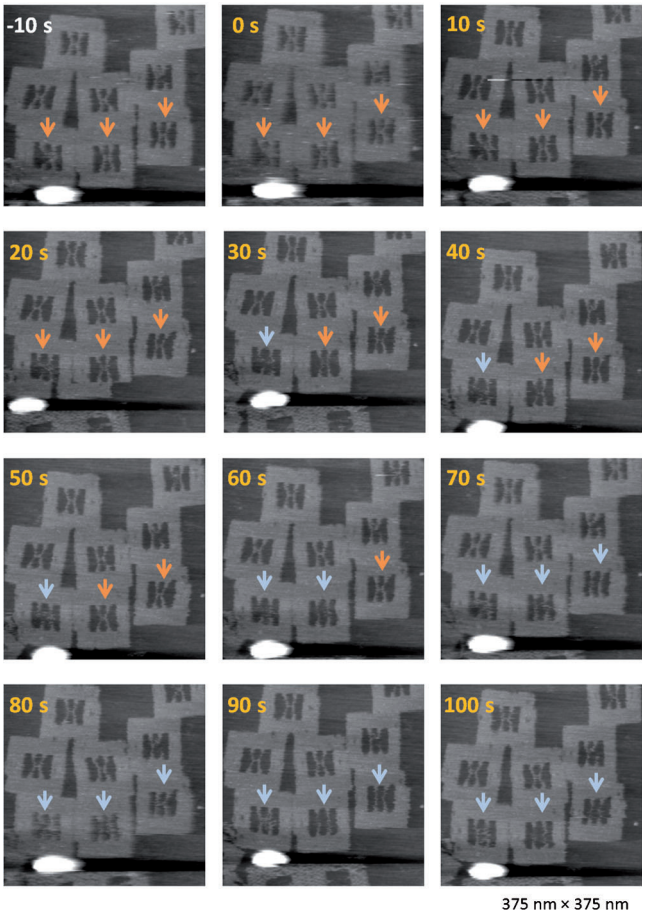

Figure 3. Dissociation of the photoresponsive domains in the DNA frame during UV irradiation. AFM scanning was 0.1 frames per second. X-shape = orange arrow; separated-shape = blue arrow.

Contact between the two dsDNAs in the middle was observed in the DNA frame during AFM scanning (Figure 4 and Movie S3). This shows that the hybridization of the two photoresponsive domains occurs following the *cis*- to *trans*-photoisomerization. In the successive AFM images, the time of the structural change from a separated-shape to an X-shape varied (100–120 s) in the individual DNA frames.

The photoisomerization of the azobenzene derivative is fast enough to be ignored when compared with the time scale for the dissociation and hybridization of the photoresponsive domains.[17] Therefore, the rate-determining process for the formation of the observed shapes should be the dissociation and hybridization of the photoresponsive domains. In these cases, the hybridization of the DNA strands requires more time as compared with the dissociation, because the hybridization requires contact and correct association of two DNA strands, a bimolecular reaction. The slower change from separated-shape to X-shape can be attributed to the slower process of hybridization between the two photoresponsive domains.

Furthermore, reversible activities of a pair of the photoresponsive domains in single DNA frame were successfully imaged under a series of UV light, visible light, UV light irradiation on the AFM stage (Figure 5 and Figure S8 and

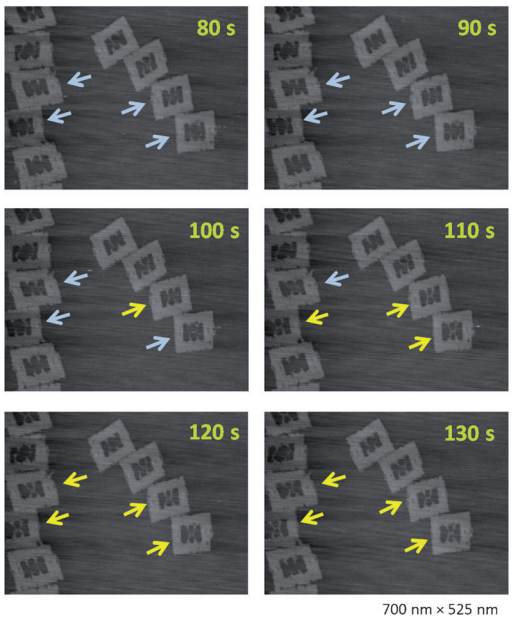

Figure 4. Hybridization of the dissociated photoresponsive domains in the DNA frame during visible-light irradiation. AFM scanning rate was 0.1 frames per second. X-shape = yellow arrow; separated-shape = blue arrow.

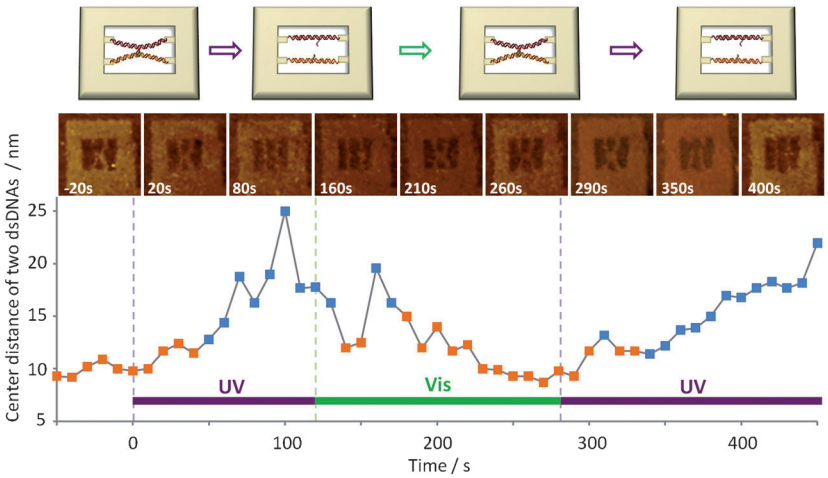

Figure 5. Photoswitching activity of photoresponsive domains in the DNA frame. Monitoring repeated dissociation and hybridization of dsDNAs during alternating UV (purple) and visible-light (green) irradiation. Irradiation was performed during AFM scanning. The distance between the centers of the two dsDNAs is plotted. X-shape = orange square; separated-shape = blue square.

Movies S4,S5). The distance between the two centers of the dsDNAs was monitored, and the alternative dissociation and hybridization of the photoresponsive domains were observed by high-speed AFM. For the first UV irradiation, dissociation of the photoresponsive domains occurred at 50 s, which was determined by its appearance and the distance between two centers of dsDNAs. During the successive visible-light irradiation, the photoresponsive domains briefly connected (140–150 s), dissociated again, and then hybridized at 180 s. This incomplete hybridization may be due to partial contact of the photoresponsive domains, which quickly dissociated again. In the second round of UV irradiation for 60 s (at 340 s in Figure 5), the duplex dissociated again. These results show that the dissociation and hybridization of the photoresponsive domains are reversible, which means that this DNA observation system can be an effective tool for observing the reversible switching behavior of single DNA duplexes.

The shape of the hybridized photoresponsive oligonucleotides was clearly visualized because both ends of the oligonucleotides were connected to the center of the two tensed dsDNAs in the DNA frame. The distance between the connection sites (**A**–**C** and **B**–**D**) in the DNA frame is approximately 15 nm, whereas the distance of the hybridized photoresponsive domains including linkers is around 10 nm. Therefore, the hybridized photoresponsive domains were supported by the tensed dsDNAs, and the straight shape of the hybridized duplex could be imaged (Figure S3). Also, the change of length of the hybridized photoresponsive oligonucleotides can be identified and the displacement of the dsDNAs is easily measured, which is an advantage to using the DNA-origami scaffold. For the photoreaction, UV irradiation sometimes causes degradation of DNA depending on the intensity and time. In this experiment, we did not observe any change in the appearance of the DNA nanostructure or dissociation of the incorporated dsDNAs in the DNA frame during UV irradiation both in solution and on the surface. The photoirradiation conditions used in this study should be weak enough to avoid much damage to the DNA.

In conclusion, we have demonstrated direct visualization of the hybridization and dissociation of photoresponsive oligonucleotides in a DNA-origami scaffold using high-speed AFM. We also have demonstrated the direct imaging of single molecular switching of the photoresponsive domains by recording the movement and global change of two dsDNAs within the DNA frame. Using UV and visible-light irradiation, we found that the dissociation and hybridization of the photoresponsive domains occurred reversibly both in solution and on the mica surface. This observation system could be used generally for investigating various DNA structural changes and molecular switches on the single-molecule level.

Experimental Section

Preparation of the DNA frame: The DNA frame structure was prepared according to a reported method.[10–12] Briefly, the DNA frame was assembled in a 20 μL solution containing M13mp18 single-stranded DNA (10 nM; New England Biolabs), staple strands (50 nM; 5 equiv.), Tris buffer (20 mM; pH 7.6), EDTA (1 mM), and $MgCl_2$ (10 mM) as shown previously.[10–12] The mixture was annealed from 85 °C to 15 °C at a rate of −1.0 °C min^{-1}.

Introduction of two dsDNAs containing photoresponsive oligonucleotides into the DNA frame: The pre-assembled dsDNAs

containing photoresponsive domains (20 nM; 2 equiv.) were incorporated into the DNA frame (10 nM) by heating at 40 °C and then cooling to 15 °C at a rate of −0.5 °C min^{-1} using a thermal cycler. The sample was purified by gel-filtration chromatography (GE sephacryl-300). The assembled structures were imaged by AFM, and the yield of incorporation was calculated manually from the AFM images.

Photoirradiation of the photoresponsive oligonucleotides within the DNA frame: Photoirradiation of the samples was performed using a Xe-lamp (300 W, Asahi spectra MAX-303) with band-pass filter (10 nm FWHM); 350 nm for UV light and 450 nm visible light. The sample containing dsDNA-attached to the DNA frame (10 nM), Tris·HCl (20 mM; pH 7.6), and $MgCl_2$ (10 mM) was irradiated in a temperature-controlled bath at 25, 30, or 35 °C for 15 min with UV and/or visible light.

High-speed AFM imaging of the dissociation and hybridization of photoresponsive oligonucleotides within a DNA frame: AFM images were obtained on a high-speed AFM (Nano Live Vision, RIBM, Tsukuba, Japan) using a silicon nitride cantilever (Olympus BL-AC10EGS). The sample (2 μL) was absorbed on a freshly cleaved mica plate for 5 min at room temperature, and then washed with the buffer solution. Scanning was performed in the same buffer solution using a tapping mode. Photoirradiation was carried out on the AFM stage (Olympus IX71 microscope) using a Hg-lamp light source (Olympus U-RFL-T) with band-pass filters (330–380 nm for UV irradiation and 440–470 nm for visible-light irradiation).

Received: July 4, 2012
Published online: September 11, 2012

Keywords: DNA origami · DNA structures · high-speed AFM · photochemistry · single-molecule observation

[1] P. V. Cornish, T. Ha, *ACS Chem. Biol.* **2007**, *2*, 53 – 61.
[2] J. Hilario, S. C. Kowalczykowski, *Curr. Opin. Chem. Biol.* **2010**, *14*, 15 – 22.
[3] C. Novo, A. M. Funston, P. Mulvaney, *Nat. Nanotechnol.* **2008**, *3*, 598 – 602.
[4] Y. Ke, S. Lindsay, Y. Chang, Y. Liu, H. Yan, *Science* **2008**, *319*, 180 – 183.
[5] N. V. Voigt, T. Tørring, A. Rotaru, M. F. Jacobsen, J. B. Ravnsbæk, R. Subramani, W. Mamdouh, J. Kjems, A. Mokhir, F. Besenbacher, K. V. Gothelf, *Nat. Nanotechnol.* **2010**, *5*, 200 – 203.
[6] T. Yoshidome, M. Endo, G. Kashiwazaki, K. Hidaka, T. Bando, H. Sugiyama, *J. Am. Chem. Soc.* **2012**, *134*, 4654 – 4660.
[7] E. Nakata, L. Fong, C. Uwatoko, S. Kiyonaka, Y. Mori, Y. Katsuda, M. Endo, H. Sugiyama, T. Morii, *Angew. Chem.* **2012**, *124*, 2471 – 2474; *Angew. Chem. Int. Ed.* **2012**, *51*, 2421 – 2424.
[8] A. Rajendran, M. Endo, H. Sugiyama, *Angew. Chem.* **2012**, *124*, 898 – 915; *Angew. Chem. Int. Ed.* **2012**, *51*, 874 – 890.
[9] T. Tørring, N. V. Voigt, J. Nangreave, H. Yan, K. V. Gothelf, *Chem. Soc. Rev.* **2011**, *40*, 5636 – 5646.
[10] M. Endo, Y. Katsuda, K. Hidaka, H. Sugiyama, *J. Am. Chem. Soc.* **2010**, *132*, 1592 – 1597.
[11] M. Endo, Y. Katsuda, K. Hidaka, H. Sugiyama, *Angew. Chem.* **2010**, *122*, 9602 – 9606; *Angew. Chem. Int. Ed.* **2010**, *49*, 9412 – 9416.
[12] Y. Sannohe, M. Endo, Y. Katsuda, K. Hidaka, H. Sugiyama, *J. Am. Chem. Soc.* **2010**, *132*, 16311 – 16313.
[13] M. Endo, K. Tatsumi, K. Terushima, Y. Katsuda, K. Hidaka, Y. Harada, H. Sugiyama, *Angew. Chem.* **2012**, *124*, 8908 – 8912; *Angew. Chem. Int. Ed.* **2012**, *51*, 8778 – 8782.
[14] H. Asanuma, X. Liang, H. Nishioka, D. Matsunaga, M. Liu, M. Komiyama, *Nat. Protoc.* **2007**, *2*, 203 – 212.
[15] X. Liang, T. Mochizuki, H. Asanuma, *Small* **2009**, *5*, 1761 – 1768.
[16] T. Ando, N. Kodera, E. Takai, D. Maruyama, K. Saito, A. Toda, *Proc. Natl. Acad. Sci. USA* **2001**, *98*, 12468 – 12472.
[17] N. Tamai, H. Miyasaka, *Chem. Rev.* **2000**, *100*, 1875 – 1890.

